K^+-NUCLEUS ELASTIC SCATTERING USING A LOCAL POTENTIAL

A.A. Ebrahim

Physics Department, Assiut University, Assiut 71516, Egypt

(Received July 7, 2001; revised version received October 10, 2001)

Kaon-nucleus scattering has been analyzed using an equivalent local potential to calculate the differential elastic, total, and reaction cross sections from ^{2}H, ^{6}Li, ^{12}C, ^{28}Si, and ^{40}Ca at kaon lab momenta ranging from 488 to 800 MeV/c. The DWUCK4 computer program was used to predict observables of kaon–nucleus scattering. Our results are successfully compared to recent data.

PACS numbers: 25.80.Dj, 25.80.Ek, 25.80.Gn

1. Introduction

The first studies of elastic scattering of K^+ from ^{12}C and ^{40}Ca gave cross sections larger than the predictions of optical model theories [1], and total cross sections for K^+ mesons on several nuclei at a range of kaon lab momenta also exceeded model expectations [2], as an indication that the nucleons within the nuclear medium do not behave as they do in free space. These observations led to several suggestions on how to remove the problem, including the interesting suggestion that medium modification such as nuclear swelling or meson mass scaling might be responsible for the lack of agreement with experimental data.

Many pion–nucleus reaction models are built on the distorted-wave impulse approximation DWIA, using the interaction of the meson with free nucleons. The DWIA pion optical potential [3,4] has been modified to treat K^+-nucleus scattering, by changing the mass of the projectile and by altering the isospin couplings in the new code DOKAY [5], to describe a range of K^+-nucleus observables.

It should be remarked here that all the previous calculations of K^+-nucleus, which are based on the impulse approximation, fall lower than the experimental data. The DOKAY code [5] with a variable Scale Factor SF multiplies the real and imaginary amplitudes for each K^+-nucleon collision

within a nucleus, representing a medium enhancement factor for K^+–N interaction. Increasing both the real and imaginary amplitudes by about 10–20% gave results nearer to the data [5]. The required enhancement for σ_R is larger than for differential elastic and inelastic scattering cross sections, this indicates that the imaginary part of K^+–N coupling needs to be enhanced as found in [6]. Reaction cross sections are almost independent of the real amplitudes, while differential elastic and inelastic scattering cross sections depend about equally on both parts of the optical potential or amplitude [5].

In the present work a quite different approach — Distorted Wave Born Approximation DWBA — is considered. It is well known that the interaction between an incident particle and a target in the Impulse Approximation, IA, is the sum of the interaction between the projectile and each individual target nucleon over all nucleons in the target nucleus, while in Born Approximation, BA, that interaction is expressed in terms of the interaction between the projectile and the whole target nucleus. In a previous work [7], the local equivalent potential together with the DWUCK4 code [8] were employed to successfully predict the angular distributions of $\pi^{\pm}$ elastically scattered from different nuclei in the (3,3) resonance region. This success motivated us to apply the same method for kaon–nucleus elastic scattering with the necessary modifications required for the present case.

Here, the angular distributions of kaons elastically scattered from ^{6}Li, ^{12}C, and ^{40}Ca at 635, 715, and 800 MeV/c kaon lab momenta are calculated using the local equivalent potential of Johnson and Satchler [9] and DWUCK4 computer code. Reaction and total cross sections for elastically scattered kaons from ^{6}Li, ^{12}C, ^{28}Si, and ^{40}Ca in the momentum range from 488 to 714 MeV/c are calculated and compared to the corresponding cross sections of Friedman *et al.* [10]. This is the first use of the DWUCK4 computer code to describe kaon–nucleus scattering within the framework of the local optical model.

Different forms of nuclear matter distribution for targets are used. In Section 2 the method employed in this work is presented while Section 3 contains results and discussion. Conclusions are presented in Section 4.

2. Method

We have used the great similarity between the pion and kaon to carry out a parallel analysis of K^+-nucleus scattering, using a local optical potential. Both mesons are pseudoscalar, and this limits their coupling with nucleons in the same way. We began with the distorted-wave Born approximation code DWUCK4 [8], since the DWUCK4 program is widely available. The DWUCK4 code solves the nonrelativistic Schrödinger equation and was

originally written to calculate the scattering and reaction observables for binary nuclear reactions.

The equivalent local potential of Johnson and Satchler [9] is used to analyze the differential elastic, total and reaction cross sections of kaons from ^{6}Li, ^{12}C, ^{28}Si, and ^{40}Ca at kaon lab momenta ranging from 488 to 800 MeV/c, where the local potentials are easier to visualize than the nonlocal versions. For the Kisslinger nonlocal potential, Johnson and Satchler [9] used the Krell–Ericson transformation, which leads from the Klein–Gordon equation for pion scattering to a local potential for the transformed wave function. Thus, a standard nonrelativistic optical model computer program may be used to calculate the angular distribution for a kaon scattered from a nucleus. Such a program should be provided with an effective kaon mass, the target mass and an effective kaon energy. The transformed wave function ψ satisfies a Schrödinger equation:

$$\{-(\hbar^2/2\mu)\nabla^2 + U_{\rm L} + V_{\rm C}\}\psi = E_{\rm c.m.}\psi\,. \tag{1}$$

$U_{\rm L}$ is the nuclear local transformed potential and is used here as follows:

$$U_{\rm L}(r) = N(U_N(r) + \Delta U_{\rm C}(r))\,, \tag{2}$$

N is the renormalization factor, the Coulomb correction term is [9]:

$$\Delta U_{\rm C} = \frac{\alpha(r)V_{\rm C} - (V_{\rm C}^2/2\omega)}{1-\alpha(r)}\,, \tag{3}$$

and the nuclear local potential is decomposed [9] into:

$$U_N(r) = U_1(r) + U_2(r) + U_3(r)\,, \tag{4}$$

where

$$\begin{aligned} U_1(r) &= \frac{(\hbar c)^2}{2\omega}\frac{q(r)}{1-\alpha(r)}, \\ U_2(r) &= -\frac{(\hbar c)^2}{2\omega}\frac{k^2\alpha(r)}{1-\alpha(r)}, \\ U_3(r) &= -\frac{(\hbar c)^2}{2\omega}\left\{\frac{\frac{1}{2}\nabla^2\alpha(r)}{1-\alpha(r)} + \left(\frac{\frac{1}{2}\nabla\alpha(r)}{1-\alpha(r)}\right)^2\right\}. \end{aligned} \tag{5}$$

The quantity $q(r)$ mainly results from the s-wave part and $\alpha(r)$ results from the p-wave part of the kaon–nucleon interaction, $q(r)$ and $\alpha(r)$ can be expressed in terms of the target nuclei density distributions and their gradients. Both are complex and energy dependent.

The predominantly s-wave interaction term $q(r)$ may be written as [9]:

$$q(r) = q_0(r) + \Delta q(r)\,, \tag{6}$$

where $q_0(r)$ is purely s-wave and is used here as:

$$q_0(r) = -4\pi p_1(b_0\rho - b_1\Delta\rho)\,, \tag{7}$$

the p-wave part of $q(r)$ is considered here as:

$$\Delta q(r) = -\tfrac{1}{2}\varepsilon\nabla^2\alpha_1(r)\,. \tag{8}$$

The p-wave part includes the Ericson–Ericson Lorentz–Lorentz (EELL) [11] correction ζ for the term linear in the density,

$$\alpha(r) = \frac{\alpha_1(r)}{1 + \frac{1}{3}\zeta\alpha_1(r)}\,, \tag{9}$$

where

$$\alpha_1(r) = \frac{4\pi(c_0\rho - c_1\Delta\rho)}{p_1}\,. \tag{10}$$

The kinematic transformation factor is $p_1 = (1+\varepsilon)$ with $\varepsilon = \omega_\circ/Mc^2$ and M is the mass of a nucleon and $\omega_\circ$ is the total energy of the kaon in the centre-of-mass system. We use ρ_n, ρ_p for the neutron, proton density distributions of the target nucleus, with $\rho = \rho_n + \rho_p$ for the total and $\Delta\rho = \rho_n - \rho_p$ for the difference; the excess neutron density. We also use $\rho_{np} = \rho^2$ as in [4]; other authors [12] replace ρ_{np} by $4\rho_n\rho_p$.

The first-order interaction parameters b_i and c_i are related to the free pion–nucleon scattering through the phase shifts $\delta_\ell(q)$ in the usual form [13],

$$\begin{aligned}
{\lambda_{s0}}^{(1)} &= \frac{4\pi}{3qk^2}p_1(2s_{31} + s_{11}),\\
b_0 &= \frac{k^2{\lambda_{s0}}^{(1)}}{4\pi p_1}\,,\\
{\lambda_{s1}}^{(1)} &= \frac{8\pi}{3qk^2}p_1(s_{31} - s_{11})\,,\\
b_1 &= \frac{k^2{\lambda_{s1}}^{(1)}}{8\pi p_1}\,,
\end{aligned} \tag{11}$$

and

$$\begin{aligned}
\lambda_{p_0}{}^{(1)} &= \frac{4\pi}{3k^3 p_1}(4p_{33} + 2p_{31} + 2p_{13} + p_{11}), \\
c_0 &= \frac{p_1 \lambda_{p_0}^{(1)}}{4\pi}, \\
\lambda_{p_1}{}^{(1)} &= \frac{8\pi}{3k^3 p_1}(2p_{33} + p_{31} - 2p_{13} - p_{11}), \\
c_1 &= \frac{p_1 \lambda_{p_1}{}^{(1)}}{8\pi},
\end{aligned} \tag{12}$$

where for s-waves ($s_{2I,2J}(q)$) and for p-waves ($p_{2I,2J}(q)$) are related to the phase shifts according to the equation:

$$s_{2I,2J}(q) \text{ (or } p_{2I,2J}(q)) = \exp[i\delta_\ell(q)] \sin \delta_\ell(q). \tag{13}$$

Here I is the total isospin of a kaon and a nucleon, J is their total angular momentum quantum number and ℓ is the orbital angular momentum quantum number. The phase shifts $\delta_\ell(q)$ are extracted from the SP92 solution of the phase shift compilation SAID code [14].

In this work, the second order interaction parameters are neglected [12] and four values of the EELL parameter are considered, namely $\zeta = 0.0$, 1.0, 1.2, and 1.8, where we used these different values of ζ to show its effect on our calculations. Here, $V_{\rm C}$ is the Coulomb potential due to the uniform charge distribution of the target nucleus of radius $R_{\rm C} = r_{\rm C} A^{1/3}$, A is the target mass number, $r_{\rm C} = 1.2$ fm [7] and $\mu = M_k m_{\rm T}/(M_k + m_{\rm T})$, where $m_{\rm T}$ is the target mass and the effective kaon mass M_k [15] is:

$$M_k = \gamma_k m_k, \tag{14}$$

where

$$\gamma_k = \frac{y + \gamma_\ell}{(1 + y^2 + 2y\gamma_\ell)^{1/2}}, y = \frac{m_k}{m_{\rm T}}, \gamma_\ell = 1 + \frac{K_\ell}{m_k c^2}.$$

K_ℓ is the kaon bombarding energy in the laboratory system and m_k is the kaon mass. Here $m_k c^2$=493.707 MeV has been used. The center-of-mass kinetic energy $E_{\rm c.m.}$ is :

$$E_{\rm c.m.} = \frac{(\hbar k)^2}{2\mu}, \tag{15}$$

with $\hbar k$ is the center-of-mass momentum of the incident kaon. The effective bombarding energy E_ℓ [15] is:

$$E_\ell = E_{\rm c.m.}(M_k + m_{\rm T})/m_{\rm T}, \tag{16}$$

which will generate the appropriate wave number k value in the form:

$$k = \left(\frac{m_k c}{\hbar}\right)\left[{\gamma_k}^2 - 1\right]^{1/2} = 4.72056 m_k [{\gamma_k}^2 - 1]^{1/2} \mathrm{fm}^{-1}\,, \qquad (17)$$

where m_k=0.53 atomic mass unit (a.u.). The kinematic parameters for the cases studied here are calculated using Eqs. (14)–(17). The resulting kinematic parameter values for the cases studied here are collected in Table I.

TABLE I

Kinematic factors for use in a nonrelativistic Schrödinger equation used in present work with kaon lab. momentum P_{lab}.

Target	P_{lab} (MeV/c)	E_{L} (MeV)	$M_k(u)$	k (fm^{-1})	p_1
^{6}Li	715	318.23	0.85304	3.155	1.6224
^{12}C	635	260.54	0.82852	3.012	1.7105
	715	307.72	0.888776	3.368	1.7586
	800	358.41	0.95457	3.751	1.8106
^{40}Ca	800	346.34	0.99142	3.955	1.9433

To show the influence of density distribution of nucleons for the considered nuclei on our calculations we used different formulae of density shape. The charge distribution of ^{6}Li was described in the form [16]:

$$\rho_{\mathrm{ch}}(r) = \frac{3}{8\pi^{3/2}}\left[\frac{1}{a^3}\exp\left(\frac{-r^2}{4a^2}\right) - \frac{c^2\left(6b^2 - r^2\right)}{4b^7}\exp\left(\frac{-r^2}{4b^2}\right)\right], \qquad (18)$$

with $a = 0.928$ fm, $b = 1.26$ fm, and $c = 0.48$ fm. Here, distributions of neutrons and protons within ^{6}Li nucleus are taken to be the same, since it is a light nucleus. We used the harmonic oscillator form for ^{6}Li and ^{12}C nuclear densities:

$$\rho_m(r) = \rho_0(1 + \alpha\left(\frac{r}{a}\right)^2)\exp\left(\frac{-r^2}{a^2}\right), \qquad (19)$$

with parameters taken from Refs. [5,17]. Also, we used the three parameter Fermi shape distribution of nucleons for ^{12}C and ^{40}Ca with parameters taken from Ref. [7]:

$$\rho_m(r) = \frac{\rho_0(1 + \omega r^2/c^2)}{[1 + \exp((r - c)/a)]}\,, \qquad (20)$$

as well as two-parameter Fermi (2PF) form which is easily obtained from the above expression of 3PF as $\omega = 0.0$. ρ_0 can be evaluated from the normalization condition:

$$\int \rho_m(r) d\bar{r} = A\,. \qquad (21)$$

3. Results and discussion

To solve Eq. (1) for kaon elastic scattering from a nucleus we employed the DWUCK4 computer code. Inserting the effective kaon mass M_k given by Eq. (14) and effective bombarding energy E_ℓ given by Eq. (16) together with the local optical potential of Ref. [9] into the DWUCK4 code to calculate kaon elastic, total and reaction cross section calculations at momenta 488, 531, 635, 656, 714, 715, and 800 MeV/c with the first-order kaon scattering parameters. The local optical potential calculations give results quite similar to recent data.

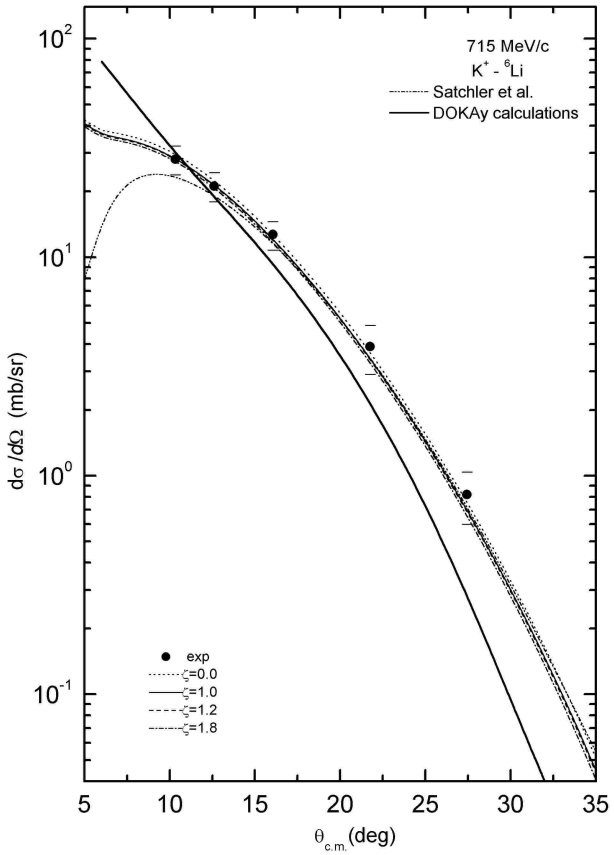

Fig. 1. $K^+-{}^6$Li differential elastic cross sections at 715 MeV/c. The dotted-, solid-, dashed-, dash-dotted curves use the harmonic oscillator distribution form and ζ=0.0, 1.0, 1.2, and 1.8, respectively represent predictions of the present work. The short dashed curve uses Eq. (19), while the thick solid curve uses DOKAY code [5]. Solid points are the experimental data taken from Ref. [18].

Using the interaction parameters for calculating the nuclear potential of elastic scattering of kaon from ^{6}Li, ^{12}C, ^{28}Si, and ^{40}Ca and inserting this potential U_{L} added to V_{C} into DWUCK4 code to generate observables such as those measured to investigate the validity of the present potential with kaons. The obtained results for best fit angular distributions of differential elastic cross section shown in Figs. 1–6 are obtained with the renormalization constant of equation (2) $N = 0.85$. The first-order parameters b_i and c_i $(i = 0, 1)$ are calculated through the phase shifts, as they are computed in the code of Ref. [5]. These parameters b_i and c_i are then used to generate the complex local potential U_{L} using the expressions from Ref. [9].

Examples are taken at momenta ranging from 488 to 800 MeV/c, where the experimental data are available. As it can be seen from Figs. 1,2,4 the EELL parameter ζ slightly affects the elastic scattering of K^{+} differential

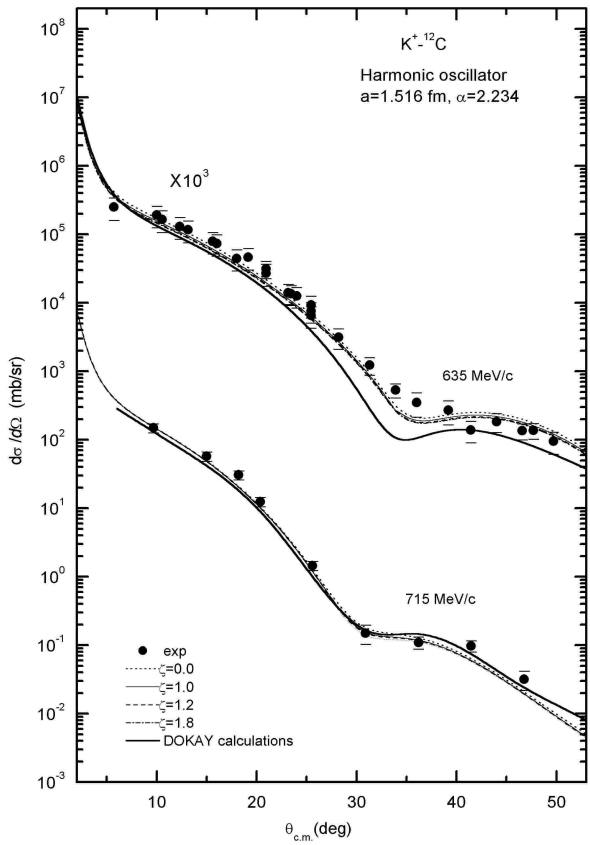

Fig. 2. As in Fig. 1 but for $K^{+}-^{12}$C differential elastic cross sections at momenta 635 and 715 MeV/c. The experimental data are taken from Ref. [18].

cross sections, this parameter was found to play a significant role in the calculations of $\pi^{\pm}$ at the (3,3) resonance region where the positions of the minima seen in the pion data were reproduced by the calculations with ζ=1.0, while these minima moved toward forward angles with the value $\zeta = 1.8$ [7].

$K^+ - {}^6$Li differential elastic cross sections have been calculated at 715 MeV/c kaon lab momentum, where the local optical potential was computed by our DWUCK4 code. The comparisons between our calculations and the experimental data of [18] are represented in Fig. 1. We have excellent agreement between our calculations and data with the two forms of

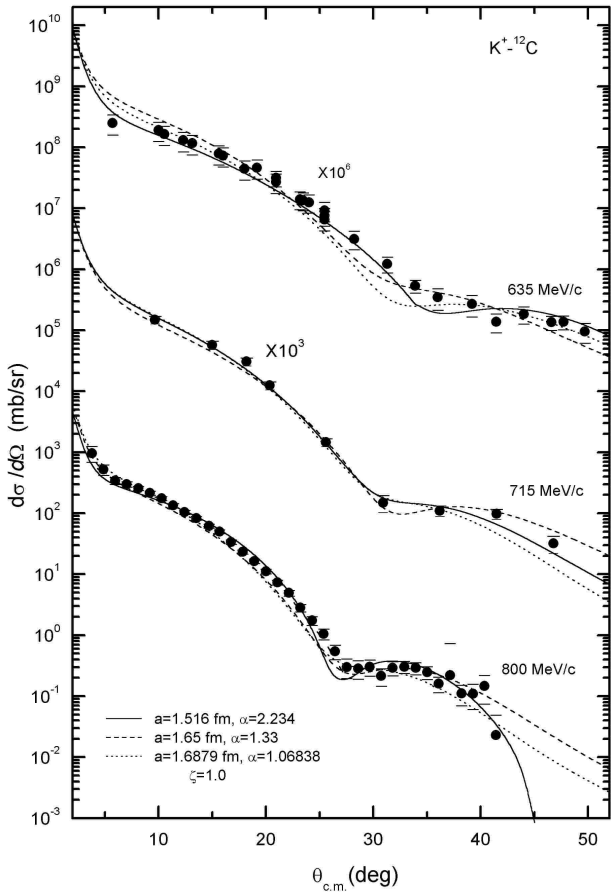

Fig. 3. $K^+ - {}^{12}$C differential elastic cross sections at different momenta 635, 715, and 800 MeV/c. The solid curves use $a = 1.516$ fm and $\alpha = 2.234$, dashed curves use $a = 1.65$ fm and $\alpha = 1.33$, and dotted curves use $a = 1.6879$ fm and $\alpha = 1.06838$, all curves use $\zeta = 1.0$. The experimental data are taken from Ref. [1, 18].

density distribution given by Eqs. (18),(19) specially at $\theta_{\text{c.m.}} \geq 12^o$, and all values of ζ=0.0, 1.0, 1.2, and 1.8. Fig. 1 shows that our predictions using the ^{6}Li density distribution given by Eq. (18) do not agree well with the experimental data at forward angles $\theta_{\text{c.m.}} < 12^\circ$ and that the EELL parameter has a negligible effect on the predicted differential cross sections. Also, shown in Fig. 1 are calculations based on DOKAY code as the thick solid curve, these calculations are lower than the data by about 30%.

Fig. 2 shows the differential elastic cross sections of K^+ from ^{12}C at 635 and 715 MeV/c. Data [18] are compared to our first order local potential calculations. The present local potential calculations using the harmonic oscillator density distribution of the form given by Eq. (19) with parameters a = 1.516 fm and α = 2.234 and the four values of ζ agree well with the

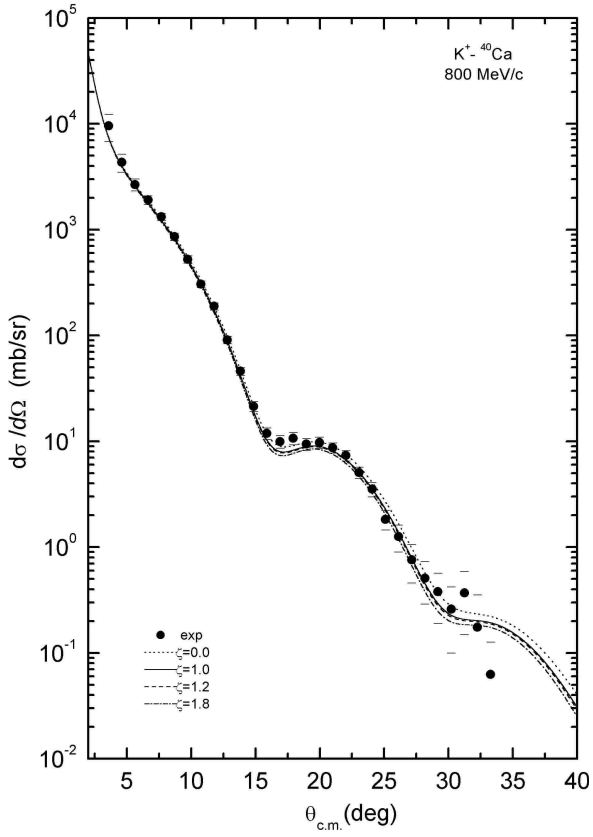

Fig. 4. As in Fig. 2, but for $K^+ - ^{40}$Ca differential elastic cross sections at 800 MeV/c using the 3PF density distributions. Solid points are the experimental data taken from Ref. [1].

data. Also calculations based on impulse approximation DOKAY code [5] are lower than the data by about 10-20%, as the thick solid curves.

In Fig. 3 we show the differential elastic cross sections of ^{12}C at 635, 715 and 800 MeV/c kaon lab momenta using different values of a and α of the harmonic oscillator density distributions. The density parameters $a = 1.516$ fm and $\alpha = 2.234$ [5] produce predictions of the present calculations shown as the solid curves better than the other values.

Fig. 4 shows the differential elastic cross sections data [1] with K^+ at 800 MeV/c from ^{40}Ca, compared to the present local optical potential calculations. We have good agreement between our calculations and data when we used the three parameter Fermi 3PF density distribution with parameters taken from [7] and the four values of ζ.

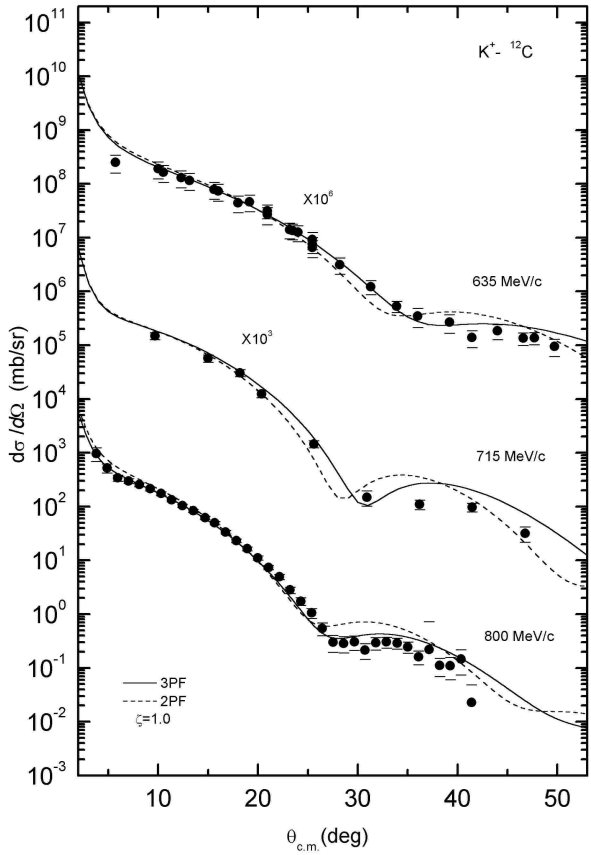

Fig. 5. $K^+ - ^{12}$C at 635, 715, and 800 MeV/c differential elastic cross sections. The solid curves use the 3PF, while the dashed curves use the 2PF density distributions. The experimental data are taken from Ref. [1, 18].

In Figs. 5, 6 we use the 2PF and 3PF density distribution of nucleons of ^{12}C and ^{40}Ca to calculate the differential cross sections for K^+ from ^{12}C and ^{40}Ca. The 3PF form as the solid curves gives results nearer to the data than does use of the 2PF form, this was found to be true when we used the local potential to describe the differential elastic cross sections of $\pi^{\pm}$ from the same nuclei [7].

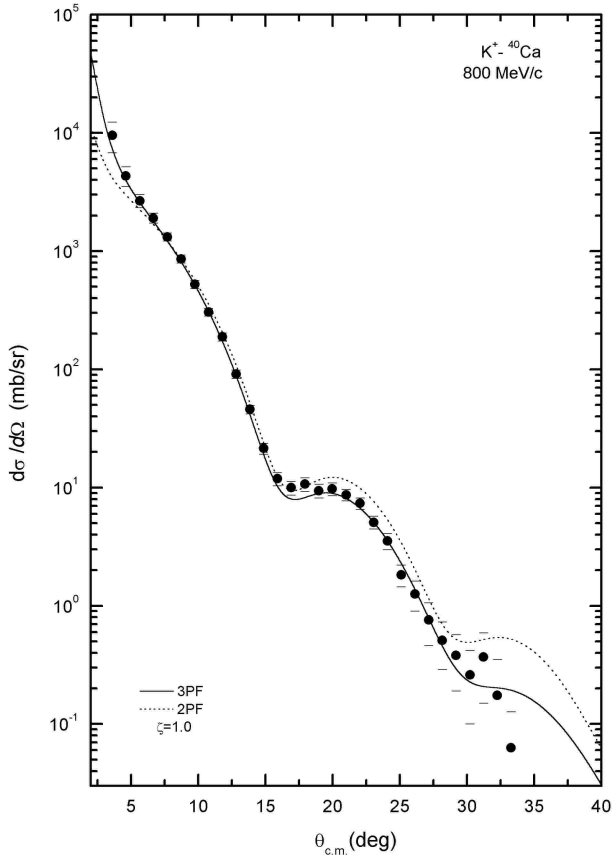

Fig. 6. As in Fig. 5, but for $K^+ - ^{40}$Ca differential elastic cross sections at 800 MeV/c. The experimental data are taken from Ref. [1].

Our first-order local optical potential is also used to predict total and reaction cross sections of kaon scattering on ^{6}Li, ^{12}C, ^{28}Si and ^{40}Ca at kaon lab momenta 488, 531, 656, and 714 MeV/c. The comparisons between our computations and Friedman *et al.* [10] are listed in Tables II, III. In Figs. 7,8 reaction and total cross sections computed by the present work as the solid curves are in better agreement with Ref. [10] than reaction and total cross sections calculated by DOKAY code [5] shown as dashed curves.

TABLE II

Reaction cross sections (in mb) for K^+ interaction with various nuclei calculated at various lab kaon momenta in MeV/c in the present work, and compared to calculations estimated by [10].

	This calculation				From Ref. [10]			
P_{Lab}	^{6}Li	^{12}C	^{28}Si	^{40}Ca	^{6}Li	^{12}C	^{28}Si	^{40}Ca
488	66.5	124.3	271.45	355.25	65.0±1.3	120.4±2.3	265.5± 5.1	349.9±7.7
531	71.5	132.4	286.35	375.45	69.8±0.8	129.3±1.4	280.4±3.4	367.1±4.5
656	77.3	144.2	309.81	409.74	75.6±1.1	141.8±1.5	306.1±3.4	401.1±5.0
714	79.5	147.3	312.65	410.35	79.3±1.2	149.3±1.5	317.5±3.6	412.9±5.5

TABLE III

As in Table II but for total cross sections for K^+ on several nuclei calculated in the present work, and compared to calculations estimated by [10].

	This calculation					From Ref. [10]				
P_{Lab}	^{2}H	^{6}Li	^{12}C	^{28}Si	^{40}Ca	^{2}H	^{6}Li	^{12}C	^{28}Si	^{40}Ca
488	26.94	79.4	167.8	379.42	498.75	25.33±0.61	76.6±1.1	162.4±1.9	366.5±4.8	494.6±7.7
531	28.03	82.4	167.9	388.88	515.72	27.15±0.32	78.8±0.7	166.6±1.3	374.8±3.3	500.2±4.4
656	28.9	89.2	176.9	400.55	533.66	28.15±0.24	84.3±0.7	174.9±0.8	396.1±2.7	531.9±4.2
714	28.97	90.1	178.3	418.66	535.76	28.65±0.20	87.0±0.6	175.6±0.9	396.5±2.3	528.4±2.8

Table IV shows the total cross section of $K^+ - ^{12}$C and K^+- deuteron. The ratio is close to 6, this means that the K^+ nucleon amplitudes are the same in ^{12}C and deuteron.

Table V shows the total K^+ cross section ratios calculated by the present work for the ^{6}Li, ^{12}C, ^{28}Si and ^{40}Ca targets. These ratios are all near unity, this reveals the near-linearity of the total cross section with mass number A. This is a property unique to K^+ mesons out of all hadronic probes in the low energy range. This indicates a volume effect and establishes the low momentum kaon as the preferred hadronic probe of nuclear matter.

TABLE IV

Total cross sections for K^+ on ^{12}C and ^{2}H nuclei calculated in the present work.

P_{Lab}	^{12}C	^{2}H	Ratio
488	167.8	26.94	6.22
531	167.9	28.03	5.99
656	176.9	28.9	6.12
714	178.3	28.97	6.15

TABLE V

Total K^+ cross sections ratios calculated in the present work for ^{6}Li, ^{12}C, ^{28}Si, and ^{40}Ca targets.

P_{Lab}	(Li/6)/(H/2)	(C/12)/(H/2)	(Si/28)/(H/2)	(Ca/40)/(H/2)
488	0.982	1.038	1.005	0.926
531	0.979	0.998	0.991	0.919
656	1.028	1.020	0.989	0.923
714	1.036	1.025	1.032	0.925

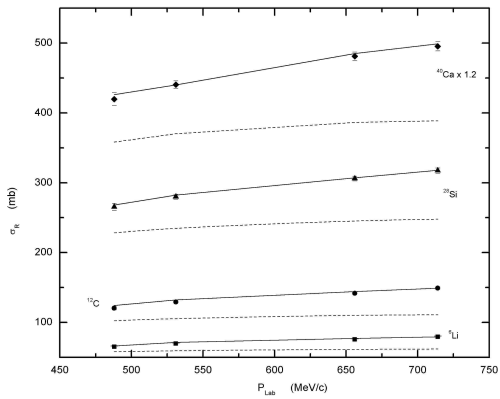

Fig. 7. Reaction cross sections for K^+ on several nuclei are shown, from Ref. [10]. Solid curves are from the present work and the dashed curves using calculations from DOKAY code [5].

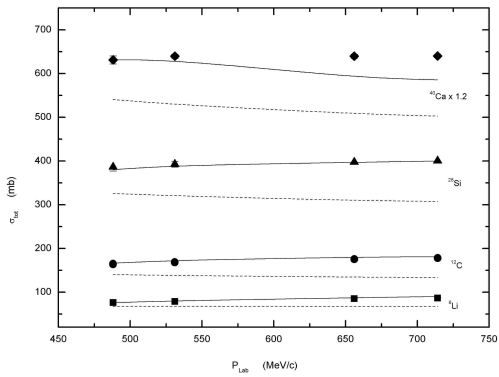

Fig. 8. As in Fig. 7, but for K^+ total cross sections on several nuclei are shown. Data are from Ref. [10].

4. Conclusions

We conclude from these calculations that the present first order renormalized local optical potential parameters using the distorted wave Born approximation DWBA, which is based on the interaction between the projectile and the whole target nucleus, with a renormalization factor < 1 give a good description for the differential, total, and reaction cross sections of kaon–nucleus elastic scattering. This fact may indicate the need for better optical potential and not enhanced in-medium K^+-nucleon cross sections or other improvements as found with free-space K^+-nucleon.

The density distributions of the nucleons by the harmonic oscillator for ^{6}Li and ^{12}C gave results nearer to the data better than the other forms of density shapes. The 3PF shape and not the 2PF of ^{12}C, ^{28}Si, and ^{40}Ca is more suitable for the nuclear density distributions of nucleons within these nuclei when they react with mesons. The EELL parameter ζ slightly affects the kaon–nucleus scattering at the momentum range considered here.

The success of this analysis of kaons elastically scattered from nuclei with the DWUCK4 program can be extended to compute the differential inelastic cross sections and the coupled channels reactions for kaons from nuclei.

I would like to thank Professor S. A. E. Khallaf, Assiut University, for his helpful discussions and careful reading of the manuscript.

REFERENCES

[1] D. Marlow *et al.*, *Phys. Rev.* **C25**, 2619 (1982).

[2] M.F. Jiang, D.J. Ernst, C.M. Chen, *Phys. Rev.* **C51**, 857 (1995); P.B. Siegel, W.B. Kaufmann, W.R. Gibbs, *Phys. Rev.* **C31**, 2184, (1985).

[3] R.A. Eisenstein, G.A. Miller, *Comput. Phys. Commun.* **11**, 95 (1976).

[4] M.B. Johnson, *Phys. Rev.* **C22**, 192 (1980); M.B. Johnson, E.R. Siciliano, *Phys. Rev.* **C27**, 1647 (1983).

[5] R.J. Peterson, A.A. Ebrahim, H.C. Bhang, *Nucl. Phys.* **A625**, 261 (1997).

[6] E. Friedman, A. Gal, J. Mares, *Phys. Lett.* **B396**, 21 (1997).

[7] S.A.E. Khallaf, A.A. Ebrahim, *Phys. Rev.* **C62**, 024603 (2000).

[8] P.D. Kunz, computer code DWUCK4, University of Colorado; P.D. Kunz, E. Rost, in *Nuclear Reactions*, *Computational Nuclear Physics*, Vol. 2 edited by K. Langanke, J.A. Maruhn, and S.E. Koonin, Springer-Verlag, New York 1993.

[9] M.B. Johnson, G.R. Satchler, *Ann. Phys.* (*N. Y.*) **248** , 134 (1996).

[10] E. Friedman *et al.*, *Phys. Rev.* **C55**, 1304 (1997).

[11] T. Ericson, W. Weise, *Pion and Nuclei*, Clarendon Press, Oxford 1988.

[12] O. Meirav, E. Friedman, R.R. Johnson, R. Olszewski, P. Weber, *Phys. Rev.* **C40**, 843 (1989).

[13] S.J. Greene, C.J. Harvey, P.A. Seidl, R. Gilman, E.R. Siciliano, M.B. Johnson, *Phys. Rev.* **C30**, 2003 (1984).

[14] R.A. Arndt, L.D. Roper, *Phys. Rev.* **D31**, 2230 (1985); *Phys. Rev.* **E46**, 961 (1992).

[15] G.R. Satchler, *Nucl. Phys.* **A540**, 533 (1992).

[16] G.R. Satchler, W.G. Love, *Phys. Rep.* **55**, 183 (1979).

[17] M.F. Vineyard, J. Cook, K.W. Kemper, M.N. Stephens, *Phys. Rev.* **C30**, 916 (1984); Shen Qing-biao, Feng Da-chun, Zhuo Yi-zhong, *Phys. Rev.* **C43**, 2773 (1991).

[18] R.E. Chrien, R. Sawafta, R.J. Peterson, R.A. Michael, E.V. Hungerford, *Nucl. Phys.* **A625**, 251 (1997).